J Intell Robot Syst (2017) 86:63–79
DOI 10.1007/s10846-016-0449-6

Analytical Inverse Kinematics Solver for Anthropomorphic 7-DOF Redundant Manipulators with Human-Like Configuration Constraints

Weihui Liu · Diansheng Chen · Jochen Steil

Received: 28 June 2016 / Accepted: 21 November 2016 / Published online: 27 December 2016

Abstract It is a common belief that service robots shall move in a human-like manner to enable natural and convenient interaction with a human user or collaborator. In particular, this applies to anthropomorphic 7-DOF redundant robot manipulators that have a shoulder-elbow-wrist configuration. On the kinematic level, human-like movement then can be realized by means of selecting a redundancy resolution for the inverse kinematics (IK), which realizes human-like movement through respective nullspace preferences. In this paper, key positions are introduced and defined as Cartesian positions of the manipulator's elbow and wrist joints. The key positions are used as constraints on the inverse kinematics in addition to orientation constraints at the end-effector, such that the inverse kinematics can be calculated through an efficient analytical scheme and realizes human-like configurations. To obtain suitable key positions, a correspondence method named wrist-elbow-in-line is derived to map key positions of human demonstrations to the real robot for obtaining a valid analytical inverse kinematics solution. A human demonstration tracking experiment is conducted to evaluate the end-effector accuracy and human-likeness of the generated motion for a 7-DOF Kuka-LWR arm. The results are compared to a similar correspondance method that emphasizes only the wrist postion and show that the subtle differences between the two different correspondence methods may lead to significant performance differences. Furthermore, the wrist-elbow-in-line method is validated as more stable in practical application and extended for obstacle avoidance.

Keywords Human-like motion · Inverse kinematics · Redundancy resolution · Correspondance problem

D. Chen (✉) · W. Liu
Robotics Institute in the School of Mechanical Engineering and Automation, Beihang University, Beijing, China
e-mail: chends@163.com

Weihui Liu
e-mail: weihui_liu@126.com

J. Steil
Institute for Robotics and Process Control, Technische Universität Braunschweig, Braunschweig, Germany
e-mail: jsteil@rob.cs.tu-bs.de

1 Introduction

Service robots, which are supposed to assist people in everyday life tasks, must be human-friendly and flexible. To improve comfort and prevent misunderstanding in human-robot interaction, the robot motion should be predictable and familiar to users or collaborating humans [1]. In the case of a redundant manipulator, there are multiple or infinitely many joint angle configurations to achieve a given end-effector task, which can be used to achieve various subtasks such as collision [2], singularity [3] and joint limit

[4] avoidance. Additionally, the redundancy can be exploited for achieving human-like behavior. The most common approaches for solving redundant inverse kinematics (IK) are iterative numerical schemes based on the Jacobian in the velocity domain [4], such as pseudo-inverse Jacobian [5] with null-space constraints and the augmented Jacobian [6]. In this paper, we propose to exploit the requirement of human-likeness in form of providing additional task space constraints. These are given as Cartesian key positions for the manipulator's elbow and wrist joints, which are used in a particularly efficient analytic scheme to solve the inverse kinematics. The proposed method is characterized by its accuracy and low computational cost for the inverse kinematics resolution. Furthermore, it is suitable for the analysis of reachable key positions in task space, especially for the case of joint limit and obstacle avoidance. It thereby lifts the advantages of solving the kinematics analytically to a relevant case of redundant human-like motion. The key positions are obtained from human demonstration and need to be mapped to the real robot in a way that respects the robot's kinematics and joint limits allowing for a valid IK solution. Thus, to perform movements in a natural and human-like fashion two separate sub-problems need to be tackled. One is to solve the inverse kinematics given key position constraints conforming to the robot's kinematics, whereas the other is to obtain suitable key postion constraints from human demonstration, which is an instance of the well-known correspondence problem.

The latter concerns the different lengths and joint limits between the human and the robot arm such that mapping the human motion directly onto the robot is not feasible. This is a persistent issue of human-like motion generation [7, 8]. Related work tried to solve the correspondence problem based on optimization schemes. In [9], Liarokapis proposed to combine individual optimization goals into a weighted global objective function. However, repeated calculation of the robot forward kinematics is neccessary. Riley et al. [10] developed a nonlinear optimization scheme to match the robot's motion to human demonstrator's. But this approach needed a good initial guess for the optimization procedure. Albrecht et al. [11] used an approach to select one cost function from a given family to approximate the given performance data best. Pollard et al. [12] focused on scaling human motion capture data to the joint and velocity range of a humanoid. Most of these optimization approaches deal with the correspondence problem in joint space.

However, also configuration parameters in operational task (Cartesian) space can be used to search for a suitable posture of the robot and to solve the inverse kinematics directly under this configuration constraint. Seraji [13] was one of the first to promote utilizing the robot redundancy for controlling the manipulator configuration directly in task space. Kim [14] kept the humanoid robot motion similar to human demonstration by sharing the same Elbow Elevation Angle (EEA), which was the key parameter of the configuration. This approach has some similarity to the one presented here, but it is less general because it was applied to a humanoid robot arm with 6-DOF and the wrist stoop angle was set to zero. Lopes et al. [15] solved the correspondence problem by finding a comfortable elbow position to keep joint positions as far away from their joint limits as possible. Liarokapis et al. [16] took the distance between robot and human elbow in task space as the criterion of anthropomorphism. Azad [17] generated an intermediate model, the Master Motor Map (MMM), to transform kinematic data between human and robot. A set of joint angles was used as configuration parameters to map the Cartesian wrist position to a natural arm posture in [18]. In [19, 20], Santis et al. considered the problem of finding a suitable configuration of the robot by adding Virtual End-effectors (VEEs) to robot arm. However, these VEEs always conflicted with each other because the constraints imposed by them outnumbered the robot's DOF. In addition, the priorities of VEEs dynamically changed during manipulation.

Approaches to directly solve the inverse kinematics under various additional constraints have also been proposed. In [21], the redundant joint value was searched for a suitable global posture to avoid collisions with the environment and then an analytical IK solver was used to rapidly compute the other six joints. In the related work [4, 16] and [22], the wrist joint of the robot was fixed according to the pose (position and orientation) of end-effector and the elbow was still free to rotate along a circular arc whose center axis was the vector from shoulder to wrist, as shown in Fig. 1. This rotation of the elbow joint without changing the pose of end-effector is called self-motion. The angle α between the plane $P_{\text{shoulder}}P_{\text{elbow}}P_{\text{wrist}}$ and the vertical plane passing through $P_{\text{shoulder}}P_{\text{wrist}}$ parameterizes the self-motion. The redundancy resolution is

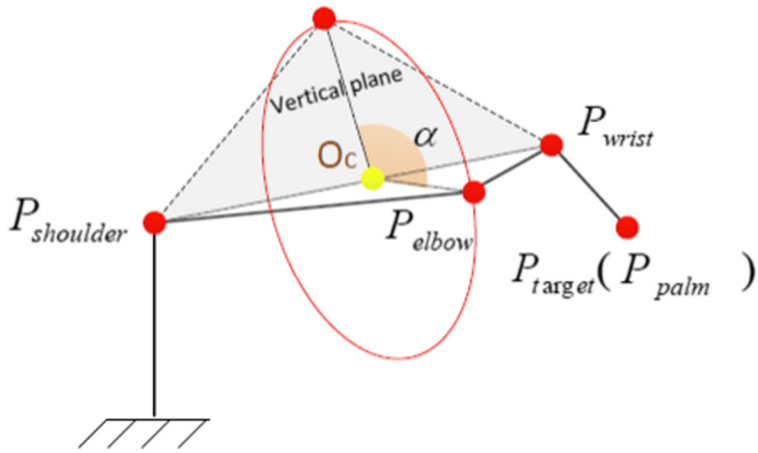

Fig. 1 Self-motion of 7-DOF robot arm with fixed wrist position. Where O_c is the rotation center of elbow joint, α is the self-motion angle

unambiguous once the self-motion angle is defined because 6 DOFs are determined already through the wrist. Then the IK solution is easily calculated analytically. Finally, in [23] a simple relationship between the hand pose and the self-motion angle was derived in the motion of the human arm, which adopted to achieve human-like motion for redundant anthropomorphic manipulators with full orientation constraints on the hand. But in everyday life tasks, often only one orientation constraint is defined at the end-effector, which frequently occurs because objects to be grasped are symmetric [8]. To grasp a beverage can, for example, only the center axis is taken into consideration during manipulation as the can is symmetric to the central axis, as shown in Fig. 2.

For a redundant robot manipulator with such partial orientation constraints, this paper contributes an analytical inverse kinematics solver and a configuration correspondence method named wrist-elbow-in-line towards generating human-like motion. To fully specify the redundancy resolution, the similarity in the kinematic structure of the human and the robot arm is utilized and encoded as Cartesian (task space) key positions in our approach. After mapping these key positions from human demonstration to the robot, which is an instance of a correspondence problem, the inverse kinematics can be solved analytically and efficiently. Because the constraints are specified in task space, they are directly and intuitively understandable for human demonstrators. Experiments are conducted to compare the correspondence method with a similar one named wrist-closest-to-human. They show, however, that subtle differences in seemingly similar ways to map the Cartesian key positions from the human to the robot may lead to significant performance differences. They highlight that one particular advantage of

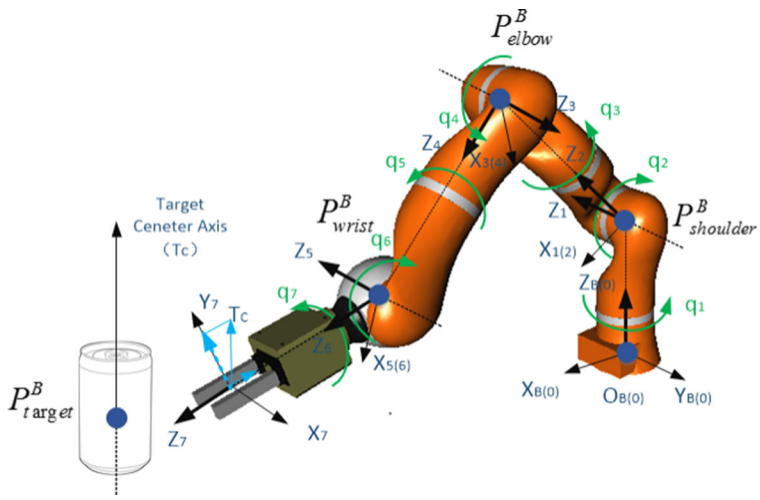

Fig. 2 Robot arm model. The revolute joint i rotates about axis Z_{i-1} with angle q_i. In the shown configuration, the joint angles $\{q_i\}$ are $\{0, -60, 0, 90, 0, 30, 90\}$, given in degrees. The projection of the target center axis T_c on axis X_7 of frame 7 equals zero

the proposed correspondence method is its flexibility in the wrist through considering only partial constraints at the end-effector. This flexibility is exploited to achieve both end-effector accuracy and human-likeness and is finally used to extend the method to include obstacle avoidance in the simulation section.

The paper is organized as follows. In Section 2, the concept of Cartesian key positions is introduced. Then the inverse kinematics solver is derived. The configuration correspondence scheme for achieving valid key positions from human demonstration is illustrated in Section 3. Experiments of Human-like motion generation are conducted in Section 4. Section 5 discusses the results of the paper and draws some conclusions.

2 Key Positions and Inverse Kinematics

This section derives the analytic resolution of the redundant inverse kinematics for 7-DOF manipulators of the type shown in Figs. 2 and 3. It assumes that constraints in form of key positions in operational Cartesian space are available for the elbow and wrist joints. It is also assumed that the end-effector is constrained only in one axis by aligning the grasp axis to the main axis of an object, as is quite common for many every-day objects [8].

2.1 Key Positions

In programming by demonstration (PbD) [24], teleoperation is a common means for recording user demonstrations [25]. The study in [26] however showed that instructing the robot arm by rotating one joint at a time felt unnatural to users and increased cognitive load. That is, controlling the robot arm in joint space to reach the desired position in task space may confuse users and may lead to misinterpretation of the robot motion. This motivates to employ key positions in task space as control parameters, which are intuitively and easy to understand for users who configure and teach the robot.

Figure 3 highlights the similarity in the kinematic structure between the human arm and the robot. We will take advantage of the fact that this type of 7-DOF serial-chain manipulators can be regarded anthropomorphic with 3-DOF at the shoulder, 1-DOF at the elbow, and 3-DOF at the wrist [27]. As shown in Fig. 3, four key positions arise naturally and lie at the intersections of joint axis. They all have a greater effect on the posture of whole robot arm, while among them the position of the shoulder is fixed to the base and the end-effector is given by the task. Thus, the configuration is determined by the positions of the wrist and the elbow, which are the main Cartesian key positions of this robot arm. Generally, for the m-DOF redundant manipulator with three position and p orientation constraints at the end-effector, the number n of main Cartesian key positions is calculated as:

$$m-3-p=\begin{cases}2n-1, & \text{if } m-p-3 \text{ is odd}\\ 2\,(n-1)\,, & \text{if } m-p-3 \text{ is even}\end{cases} \tag{1}$$

For the 7-DOF robot arm with three position and one orientation constraints at the end-effector, there are two main key positions for wrist and elbow.

2.2 Robot Arm Model

The seven revolute joints of the robot arm are represented by joint variables $q_1,\ldots,q_7$, which parametrize the rotation about axis Z_{i-1} in coordinate system $i-1$ respectively. As shown in Fig. 2, the base coordinate system (B) is fixed to the ground. DH parameters are used to describe the homogeneous transforms between successive coordinate systems and are listed in Table 1.

Denote by A_i^j the coordinate transform of the i-th coordinate system with respect to a reference coordinate system j. This allows to express coordinates of points in a coordinate system k with respect to the base coordinate system B as:

$$P^{\mathrm{B}}=A_k^{\mathrm{B}}P^k \tag{2}$$

2.3 Inverse Kinematics

The inverse kinematics of the redundant manipulator will have a unique solution if Cartesian key position constraints respecting the robot's kinematics are given. Then the IK can be calculated by means of an efficient analytical scheme. First, the elbow position depends only on the rotation of joints 1 and 2. Thus these two joint angles can be calculated according to the elbow key position of robot. If q_1 and q_2 are known, the position of wrist depends only on the rotation of joint 3 and joint 4. Then q_3 and q_4 can be obtained if the wrist key position of robot is known. These relationships between key positions and joint angles are listed in Table 2, where the joint angles in

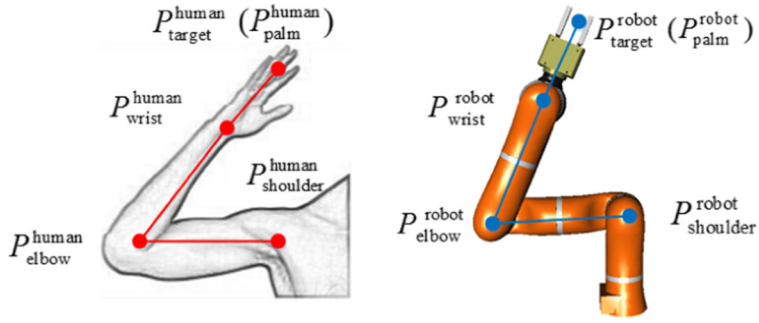

Fig. 3 Human and robot arm kinematic structures, and key positions of them

round brackets '( )' are assumed to be known respectively. Finally, T_c denotes the orientation of the target center axis, as shown in Fig. 2.

We now elaborate the respective computations. As shown in Eq. 3, q_1 and q_2 can be found for given elbow position with respect to the base frame $P^{\mathrm{B}}_{\mathrm{elbow}} = [P^{\mathrm{B}}_{\mathrm{elbow}}.x,\ P^{\mathrm{B}}_{\mathrm{elbow}}.y,\ P^{\mathrm{B}}_{\mathrm{elbow}}.z]^T$, where $P^{\mathrm{B}}_{\mathrm{elbow}}.x$, $P^{\mathrm{B}}_{\mathrm{elbow}}.y$, $P^{\mathrm{B}}_{\mathrm{elbow}}.z$ are the x, y, z coordinate values of the elbow joint in the base frame, and $P^{3}_{\mathrm{elbow}} = [0, 0, 0, 1]^T$ is the origin of frame 3 (elbow joint).

$$P^{\mathrm{B}}_{\mathrm{elbow}} = A^{\mathrm{B}}_{3} P^{3}_{\mathrm{elbow}} = A^{B}_{1} A^{1}_{2} A^{2}_{3} P^{3}_{\mathrm{elbow}}$$

$$\begin{bmatrix} P^{\mathrm{B}}_{\mathrm{elbow}}.x \\ P^{\mathrm{B}}_{\mathrm{elbow}}.y \\ P^{\mathrm{B}}_{\mathrm{elbow}}.z \\ 1 \end{bmatrix} = \begin{bmatrix} -l_2 \cos(q_1) \sin(q_2) \\ -l_2 \sin(q_1) \sin(q_2) \\ l_1 + l_2 \cos(q_2) \\ 1 \end{bmatrix} \tag{3}$$

Therefore,

$$\begin{aligned} \cos(q_2) &= (P^{\mathrm{B}}_{\mathrm{elbow}}.z - l_1)/l_2 \\ \sin(q_2) &= \pm\sqrt{1 - \cos(q_2)^2} \end{aligned} \tag{4}$$

$$q_1 = \mathrm{a\,tan\,2}(\pm P^{\mathrm{B}}_{\mathrm{elbow}}.y, \pm P^{\mathrm{B}}_{\mathrm{elbow}}.x) \tag{5}$$

The signs in Eq. 5 are opposite to $\sin(q_2)$. q_3, q_4 are calculated in a similar way.

$$P^{\mathrm{B}}_{\mathrm{wrist}} = A^{\mathrm{B}}_{5} P^{5}_{\mathrm{wrist}} = A^{B}_{1} A^{1}_{2} A^{2}_{3} A^{3}_{4} A^{4}_{5} P^{5}_{\mathrm{wrist}} \tag{6}$$

$$\begin{aligned} &(A^{1}_{2})^{-1} (A^{\mathrm{B}}_{1})^{-1} P^{\mathrm{B}}_{\mathrm{wrist}} = A^{2}_{3} A^{3}_{4} A^{4}_{5} P^{5}_{\mathrm{wrist}} \\ &\begin{bmatrix} m \\ n \\ p \\ 1 \end{bmatrix} = \begin{bmatrix} l_3 \cos(q_3) \sin(q_4) \\ l_3 \sin(q_3) \sin(q_4) \\ l_2 + l_3 \cos(q_4) \\ 1 \end{bmatrix} \end{aligned} \tag{7}$$

$P^{5}_{\mathrm{wrist}} = [0, 0, 0, 1]^T$, is the origin of frame 5 (wrist joint). Similarly,

$$\cos(q_4) = (p - l_2)/l_3 \tag{8}$$

$$q_3 = \mathrm{a\,tan\,2}(\pm n, \pm m) \tag{9}$$

Then q_5 and q_6 are obtained by solving the following equations:

$$P^{\mathrm{B}}_{\mathrm{target}} = A^{B}_{7} P^{7}_{\mathrm{target}} = A^{B}_{1} A^{1}_{2} A^{2}_{3} A^{3}_{4} A^{4}_{5} A^{5}_{6} A^{6}_{7} P^{7}_{\mathrm{target}} \tag{10}$$

$$(A^{3}_{4})^{-1} (A^{2}_{3})^{-1} (A^{1}_{2})^{-1} (A^{B}_{1})^{-1} P^{\mathrm{B}}_{\mathrm{target}} = A^{4}_{5} A^{5}_{6} A^{6}_{7} P^{7}_{\mathrm{target}} \tag{11}$$

Table 1 DH Parameters of Kinematic Model

i	α_{i-1}	a_{i-1}	d_i	θ_i	joint limit
1	$\pi/2$	0	l_1	q_1	$\pm 170°$
2	$-\pi/2$	0	0	q_2	$\pm 120°$
3	$-\pi/2$	0	l_2	q_3	$\pm 170°$
4	$\pi/2$	0	0	q_4	$\pm 120°$
5	$\pi/2$	0	l_3	q_5	$\pm 170°$
6	$-\pi/2$	0	0	q_6	$\pm 120°$
7	0	0	l_4	q_7	$\pm 170°$

Table 2 Correspondence between Key Positions and Joint Angles

Key Positions	Joint Angles
$P_{\text{elbow}}^{\text{robot}}$	q_1, q_2
$P_{\text{wrist}}^{\text{robot}}$	$(q_1, q_2), q_3, q_4$
$P_{\text{hand}}^{\text{robot}}$ (P_{target})	$(q_1, q_2, q_3, q_4), q_5, q_6$
Target Center Axis T_c	$(q_1 \cdots q_6), q_7$

Because the variables on the left hand side of Eq. 11 are already known through previous calculation, q_5 and q_6 are found in the same way as shown before.

The joint angle q_7 describes the end-effector rotation about the OZ axis in frame 7 (target). Suppose that the projection of the target center axis T_c on the plane XOY in frame 7 is collinear with the coordinate axis Y_7, as the dashed vector in Fig. 2. Then the projection of T_c on axis X_7 equals zero.

$$T_c{}^7 = A_B^7 T_c{}^B = A_6^7 A_5^6 A_4^5 A_3^4 A_2^3 A_1^2 A_B^1 T_c{}^B \tag{12}$$

$$\begin{gathered}(A_6^7)^{-1} T_c{}^7 = A_7^6 T_c^7 = A_5^6 A_4^5 A_3^4 A_2^3 A_1^2 A_B^1 T_c{}^B \\ \begin{bmatrix} T_c{}^7.y \sin(q_7) \\ T_c{}^7.y \cos(q_7) \\ T_c{}^7.z \\ 0 \end{bmatrix} = \begin{bmatrix} m \\ n \\ p \\ 0 \end{bmatrix}\end{gathered} \tag{13}$$

Where $(A_m^n)^{-1} = A_n^m$, $T_c{}^7 = [0, T_c{}^7.y, T_c{}^7.z, 0]^T$ and $T_c = T_c{}^B = [T_c{}^B.x, T_c{}^B.y, T_c{}^B.z, 0]^T$. Because only the rotation is taken into consideration for solving q_7, set the last entries of vectors $T_c{}^7$ and $T_c{}^B$ to zero to avoid a translation of the coordinate origin. Then q_7 is easily obtained from Eq. 13.

3 Configuration Correspondence

Human demonstration data needs to be mapped to the real robot, because the latter may have different link lengths and joint limits. This section addresses this correspondence problem. It assumes that Cartesian key positions are given from human demonstration as shown in Fig. 4 and have already translated and scaled into the robot workspace. Then the shoulder key positions of the human and the robot coincide and the target axis T_c is aligned as shown in Fig. 2. It remains to find respective elbow and wrist key positions for the robot from the key position of human. These have to be suitable for the analytic solution of the IK solver in the sense that they respect the link lengths and joint limits of robot.

3.1 Correspondence Method

There is evidence from previous work [14, 28] that the elbow position is an important parameter for the configuration of human-like manipulators. In the case of a fully constraint end-effector, the wrist position is defined by the pose of the end-effector. As shown in Fig. 1, the plane formed by shoulder, elbow and wrist is used to describe the posture of the arm, which can freely rotate about the connection line between the shoulder and the wrist [13]. This rotation is parametrized by the self-motion angle. Then the criterion to find a human-like configuration of the robot is to keep elbows of the robot and the human in the same plane by adjusting the self-motion angle. For the partial orientation constraints at the end-effector that are considered here, the wrist key position of robot can additionally move along the surface of a sphere centered at the end-effector. Thus the natural generalization of the standard method described above is to use the plane formed by the shoulder, elbow and palm of human as reference plane and to position the robot elbow accordingly. We describe this method in more detail next.

We assume that the elbow of robot falls on the reference plane and suppose the wrist of robot is determined by the direction from the palm to the wrist of human, which is closest to the human wrist (wrist-closest-to-human, see Fig. 5). So usually there are two solutions for the robot elbow position. The one closer to human elbow is chosen as the elbow of robot. However, in this approach it is easy to reach the joint limit of the robot. Take the case of Fig. 5a, for instance, where q_4 exceeds its joint limit (± 120 degree for Kuka-LWR) because of the different lengths and joint limits between the human and the robot arm. Fluctuating demonstration data may even aggravate this problem. For example, when the captured wrist position of human cannot match the real one in Fig. 4b, the offset error of captured data causes q_6 to reach its joint limit easily, as shown in Fig. 5b. And inaccurate captured key positions of human demonstrations can also cause the length of the human arm to differ significantly from the length of the robot. An example is shown in Fig. 5c, where the length of the robot's palm

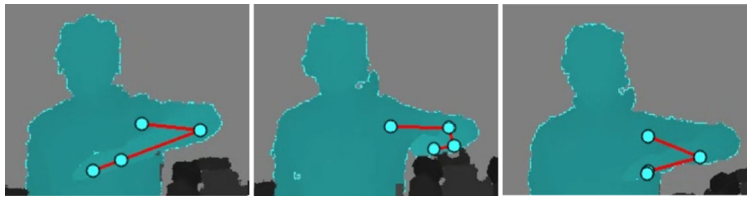

(a) accurate (b) inaccurate wrist (c) inaccurate wrist and elbow

Fig. 4 Key positions of human demonstration. (**a**) Points are derived from motion capture as shoulder, elbow, wrist and palm (target) key positions. (**b**) shows that the captured wrist position of the human demonstration cannot match the real one. And both captured wrist and elbow position of human demonstration drift in (**c**)

is longer than the length of the human forearm. Then the robot elbow position, which is closer to the human elbow on the reference plane, points to the direction opposite of the natural posture and reaches the joint limits of q_2 and q_6. These problems are notorious and can easily occur if low quality human demonstration data are processed, for instance from a Kinect. We conclude that this generalization of the direct classical elbow-angle method is not very robust and a different method is needed, which is also confirmed by the experimental results in Section 4.

We therefore propose a further correspondence method for partial constraints at the end-effector that is inspired by the lazy manipulation of the human example. As shown in Fig. 4, the real palm, wrist and elbow key positions of human tend to stay in line naturally, which expends as little energy as possible. Accordingly, we propose to choose the robot key positions such that the wrist key position is on the connection line between palm and elbow (wrist-elbow-in-line) and that all of the key positions fall on the reference plane. In this case, q_6 equals zero at the position farthest away from its joint limits. This also happens in its singularity which can be handled by the robot controller and by the configuration adjustment procedure described later. This makes the wrist flexible for further adjustment such as obstacle and joint limit avoidance. And the elbow is on the reference plane pointing to the direction of the human elbow which sustains the human-like configuration. The process of how to get the robot key positions is illustrated in Fig. 6. When the robot elbow and wrist are in line, the palm, elbow and shoulder of robot form a triangle that has two sides with fixed length, palm to elbow and elbow to shoulder. Then the elbow key position of robot can be calculated depending only on the position of palm. Finally, the wrist key position of robot is easy to obtain. Note that key positions of the robot must be preprocessed and be adjusted for a valid IK solution in case of joint limit or obstacle avoidance. Essentially, the elbow key position of robot should fall on the reference plane to keep the human-like posture of the robot arm and the wrist key position must be flexible to guarantee the existence of a solution for the elbow in the reference plane with reachable joints angles.

3.2 Configuration Adjustment

The robot key positions obtained in the previous section through either method are assigned as the initial key positions of robot. Then the robot key

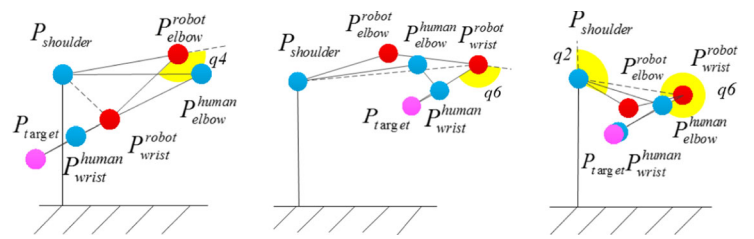

(a) accurate: q_4 out of limit (b) inaccurate wrist: q_6 out of limit (c) inaccurate wrist and elbow: q_2 and q_6 out of limit

Fig. 5 Correspondence method with the wrist key position of robot in the direction from the human palm (target) to the human wrist (wrist-closest-to-human). Key positions correspond to the human demonstration shown in Fig. 4

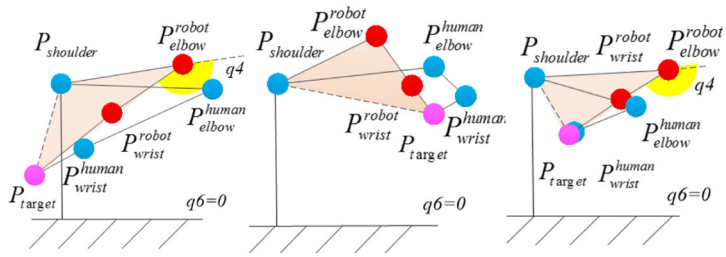

(a) accurate: q_4 out of limit (b) inaccurate wrist (c) inaccurate wrist and elbow: q_4 out of limit

Fig. 6 Correspondence method with the wrist key position of robot in line with the robot elbow (wrist-elbow-in-line). Key positions correspond to the human demonstration shown in Fig. 4

positions for both correspondence methods can be iteratively adjusted to avoid joint limits until a valid IK solution can be computed by the method presented in Section 2. There are two major steps.

Algorithm 1 Configuration Adjustment

Require: $P^{\text{human}}_{\text{wrist}}$,$P^{\text{human}}_{\text{elbow}}$

1: Calculate initial key positions of robot with regard to different correspondence method : $(P^{\text{robot}}_{\text{wrist}})^{\text{initial}}$,$(P^{\text{robot}}_{\text{elbow}})^{\text{initial}}$
2: **while** q_4 exceeds joint limit **do**
3: rotate $P^{\text{robot}}_{\text{wrist}}$ in the plane $P_{\text{palm}}P^{\text{robot}}_{\text{wrist}}P_{\text{shoulder}}$ to make robot wrist away from shoulder
4: calculate new robot wrist $(P^{\text{robot}}_{\text{wrist}})^{\text{new}}$
5: calculate new robot elbow in the reference plane $(P^{\text{robot}}_{\text{elbow}})^{\text{new}}$
6: **end while**
7: **while** q_2 or q_6 exceeds joint limit **do**
8: rotate $P^{\text{robot}}_{\text{elbow}}$ about the vector from P_{shoulder} to $P^{\text{robot}}_{\text{wrist}}$
9: calculate new robot elbow $(P^{\text{robot}}_{\text{elbow}})^{\text{new}}$
10: **end while**

The first step is to adjust the wrist key position of robot to obtain a feasible q_4. Reachable positions of the robot wrist are distributed on the blue sphere whose center is the target position of robot with a radius of l_4 as shown in Fig. 7a. q_4 is determined by the position of the wrist because two sides of the triangle formed by the shoulder, elbow and wrist of robot are fixed as l_2 and l_3 (in Fig. 7a). The relationship between q_4 and the length of $\left|P_{\text{shoulder}}P^{\text{robot}}_{\text{wrist}}\right|$ is:

$$\left|P_{\text{shoulder}}P^{\text{robot}}_{\text{wrist}}\right| = \sqrt{{l_2}^2 + {l_3}^2 - 2l_2l_3\cos\left(\pi - |q_4|\right)} \tag{14}$$

This is consistent with the correspondence relationship between key positions and joint angles in Table 2. If the current q_4 exceeds the joint limit($\pm 120°$), then the wrist key position of robot needs to rotate in the green plane formed by the shoulder, wrist and palm of the robot by an amount θ about the normal vector $\vec{n}$. Each such iterative step will drive the wrist of robot away from the robot shoulder. The intersection circle (dotted line) of this plane and the reachable sphere of the robot wrist are possible solutions for the position of the robot wrist in Fig. 7a and b. Note that possible positions of the robot wrist fall in the reference plane if the wrist is assumed to be in line with elbow. $\vec{v}$ is the unit vector from the robot palm to the current wrist. Then the new wrist position $(P^{\text{robot}}_{\text{wrist}})^{\text{new}}$ can be obtained according to Rodrigues' rotation formula [29] in each iterative step:

$$\vec{v}_{\text{new}} = \vec{v}\cos\theta + (\vec{n}\times\vec{v})\sin\theta + \vec{n}(\vec{n}\cdot\vec{v})(1-\cos\theta) \tag{15}$$

$$(P^{\text{robot}}_{\text{wrist}})^{\text{new}} = P_{\text{palm}} + l_4\vec{v}_{\text{new}} \tag{16}$$

Once the wrist key position of robot is obtained, the robot elbow can only rotate about the vector from robot shoulder to wrist. The position on the reference plane that is closer to the human elbow is chosen as the new elbow key position of robot. After adjustment as above, the robot wrist features a valid inverse kinematic solution for q_4 as shown in Fig. 7b. Beyond that, the robot elbow is in the reference plane, which meets the requirement of a human-like configuration.

Secondly, if q_2 or q_6 exceeds the joint limit, the elbow key position of robot needs to rotate until the joint value valid within the joint limits in order to avoid repeating or reversing the previous modification of q_4. The possible solutions of the robot elbow are

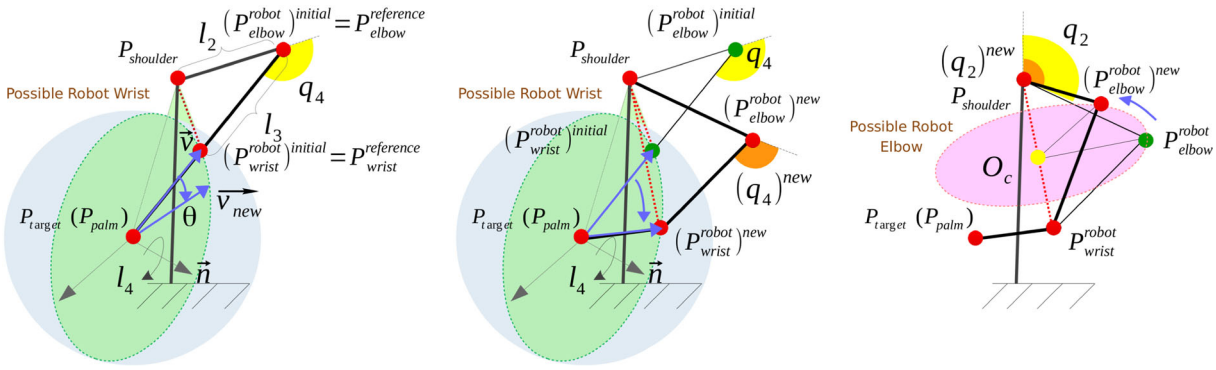

Fig. 7 Configuration Adjustment. Points in green and red are key positions of robot in the last and current step, respectively. Possible robot wrist and elbow positions lie on the dotted circle centered at target (palm) and O_c. (**a**) is in the case that q_4 exceeds joint limit,(**b**) is about the adjustment of wrist key position and (**c**) is about adjustment of elbow key position searching for reachable q_2

distributed as the red dotted line arc in Fig. 7c and can be obtained similar to Eqs. 15 and 16. Note that after the rotation of the robot elbow to obtain a valid IK solution, the posture of robot may be not as similar to the human demonstration as before.

4 Simulation

In this part, we evaluate the accuracy of the inverse kinematics solver and the human-likeness of the correspondence method. To this aim, the robot arm is required to follow the motion of a human demonstration in real time. Finally, the correspondence approach is combined with obstacle avoidance to test its flexibility. The experimental system and simulation results are presented in following sections.

4.1 Experiment System

The proposed method is applied to control the configuration of the Kuka-LWR robot arm model in real time through human demonstration. The framework of this system is shown in Fig. 8, where q represent values of joint angle and P^*_{key} are the key positions in the coordinate system *. The skeleton data of the human motion are captured using Kinect. Before application of the correspondence procedure, a scaling step is performed to address the issue of length and coordinate system differences between the human and the robot arm. The ratio between the robot and the human arm length is multiplied with the human demonstration data in order to fit the workspace of the robot. As shown in Fig. 9, the coordinate transformation from robot to the visual system is:

$$A^{\text{robot}}_{\text{kinect}} = T_Z(l_1)R_Z(-\pi/2)R_X(\pi/2) \tag{17}$$

$$P^{\text{robot}}_{\text{human}} = A^{\text{robot}}_{\text{kinect}} P^{\text{kinect}}_{\text{human}} \tag{18}$$

Then key positions of the human are mapped onto the robot through configuration correspondence and the analytical inverse kinematic solver is engaged, which solves the redundant inverse kinematic problem by finding suitable postures and configuration of the robot in task space. The experimental system is supported by the Research Institute for Cognition and Robotics (CoR- Lab) [30, 31].

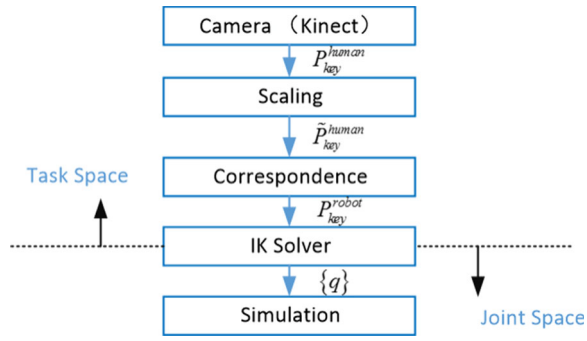

Fig. 8 Experimental system structure overview

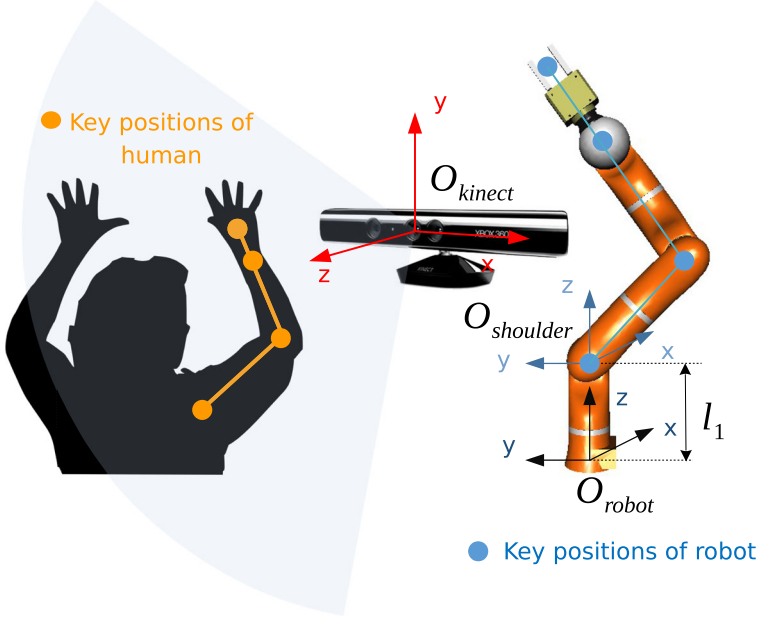

Fig. 9 Coordinate systems of human, robot and camera

4.2 Real-time Tracking of Human Demonstartion

The first experiment is conducted to compare the robot's ability of human-like motion generation with regard to the two correspondence methods. Namely, the wrist-closest-to-human method proposed in Fig. 5, in which the wrist key position of robot is in the direction from human palm to human wrist, and the wrist-elbow-in-line method proposed in Fig. 6, in which wrist key position of robot is line with robot elbow.

(a) Captured human demonstration

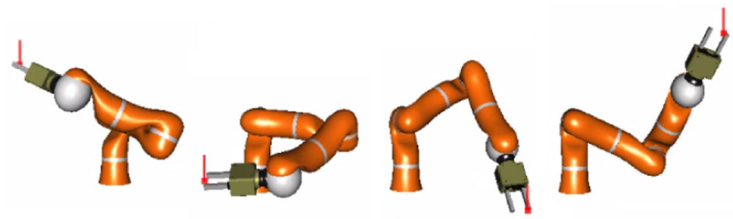

(b) Generated motion by wrist-elbow-in-line correspondence method

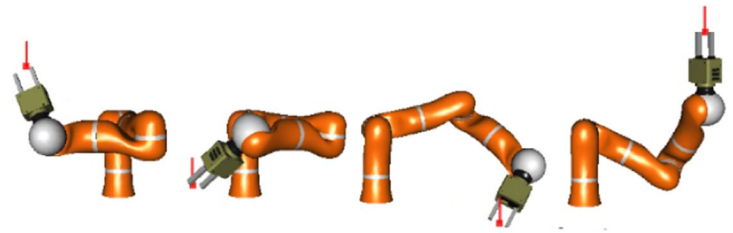

(c) Generated motion by wrist-closest-to-human correspondence method

Fig. 10 The robot follows the motion of the human in the case that captured key positions of human demonstration cannot match the real human motion. The red point in (**b**) and (**c**) is the end-effector position mimicking the human palm. The captured palm positions have an offset error in both the *first* and the *second column*. And the captured wrist and elbow positions cannot match the real one in the *third* and *last column*

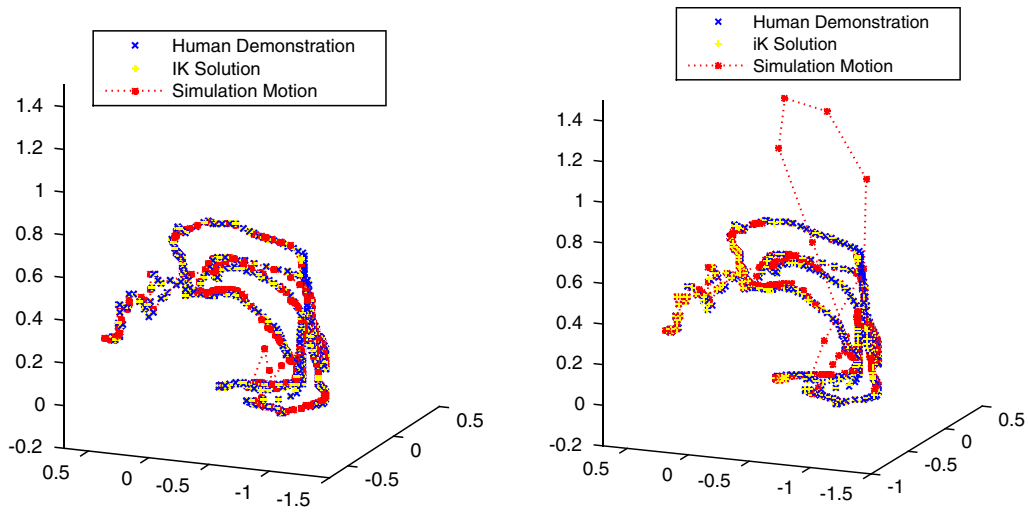

(a) Generated trajectory by wrist-elbow-in-line correspondence method.

(b) Generated trajectory by wrist-closest-to-human correspondence method.

Fig. 11 Comparison of end-effector trajectories for the different correspondence methods

The robot is tracking the human palm trajectory captured by the Kinect depth camera in real time, while imitating the posture of the human arm. From an intuitive point of view in Fig. 10, both correspondence methods can enable the end-effector of robot to follow the position of human palm and generate human-like motion by keeping the elbow of robot and the elbow of human in the same plane ($P_{\text{shoulder}} P_{\text{elbow}}^{\text{human}} P_{\text{palm}}$), even in the case that captured key positions of the human cannot match the real human motion.

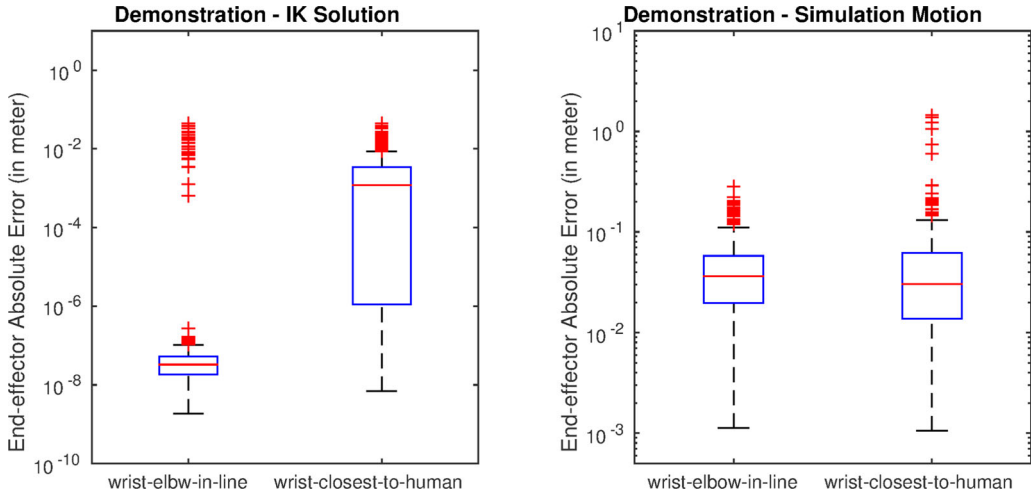

(a) End-effector accuracy of IK solver solution.

(b) End-effector accuracy of simulation motion.

Fig. 12 Accuracy evaluation for IK solver based on the different correspondence methods

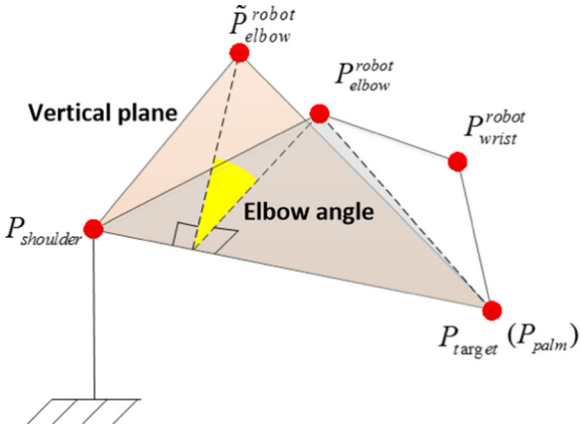

Fig. 13 Elbow angle of robot arm

However, the results show that the unstable and fluctuating capture data affect the wrist position generated by wrist-closest-to-human more significantly.

4.2.1 Accuracy Analysis of End-effector Tracking

For both methods, the 3-dimensional end-effector trajectories are plotted in Fig. 11 and qualitatively show an excellent tracking of the human data by visual inspection, especially for wrist-elbow-in-line method. Also a quantitative accuracy evaluation is performed and shown in Fig. 12. When the current joint value is near its limit, abrupt changes of the robot configuration are possible as the arc-shape trajectory on the top of Fig. 11b shows. This causes large errors up to 1 meter, nearby on the right of Fig. 12b. Because of the velocity limitations of the simulation system (see [31]) which is identified with the real Kuka arm, there is a slight delay between the human and simulated robot motion. That is the reason that for both methods the calculated solution of the IK solver has higher accuracy than the simulated end-effector motion (Fig. 12). And loss of precision might also occur if no valid corresponding IK solution for the robot key positions is found, because if the joint is out of its reachable range it is set to its limit value. Also, the wrist-closest-to-human method easily reaches the joint limits of q_2 and q_6. Consequently, the error of this method (mean of 0.0034 meter for IK solution and 0.0535 meter for simulated motion) is larger than the that of wrist-elbow-in-line method (mean of 0.0007 meter for IK solution and 0.0459 meter for simulated motion).

4.2.2 Human-likeness Analysis of Posture

Similar to the self-motion angle in Fig. 1, for partial orientation constraints at the end-effector the angle between the robot plane $P_{\text{shoulder}}P^{\text{robot}}_{\text{elbow}}P_{\text{palm}}$ and the vertical plane passing through $P_{\text{shoulder}}P_{\text{palm}}$ parameterizes the motion and serves as elbow angle (see

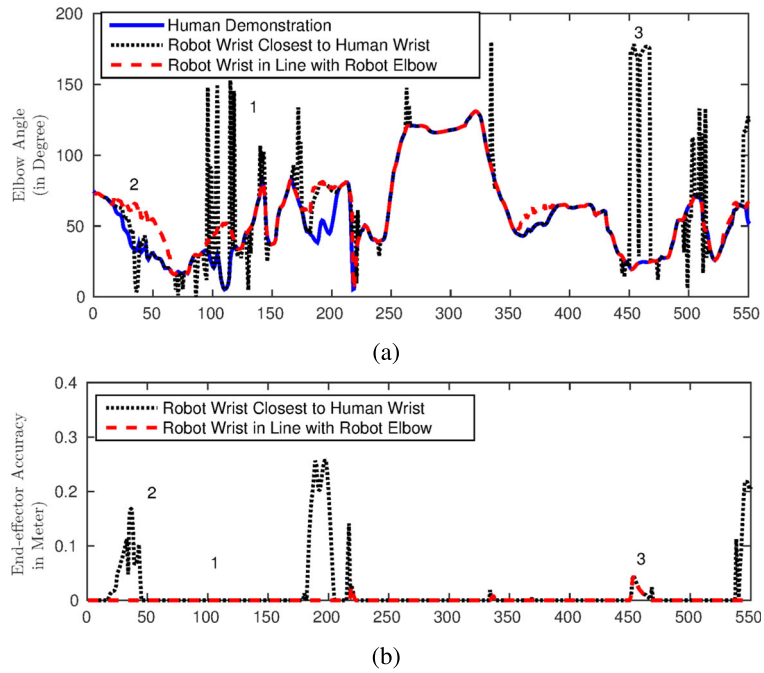

Fig. 14 Comparison between correspondence methods: the robot's wrist closest to the wrist of human (*wrist-closest-to-human*) vs. in line with the elbow of robot (*wrist-elbow-in-line*). (**a**) and (**b**) show the elbow angle and the end-effector accuracy comparison respectively

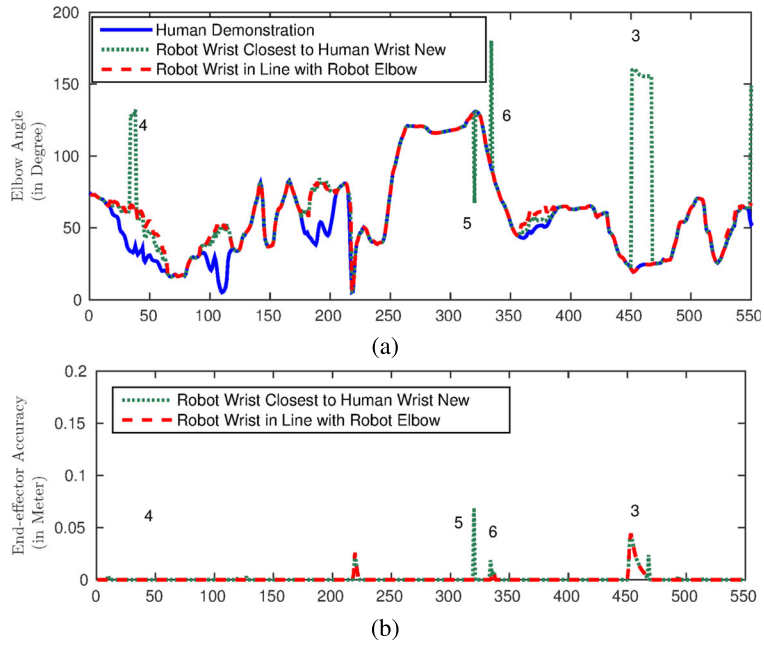

Fig. 15 Comparison between correspondence methods: human's elbow used instead of the wrist for the wrist-closest-to-human method vs. the robot's wrist in line with the wrist of robot (*wrist-elbow-in-line*). (**a**) and (**b**) show the elbow angle and the end-effector accuracy comparison respectively

Fig. 13). Good human-likeness is evaluated as similarity of the elbow angle value between the robot and the human demonstration. Figs. 14–16 compare the ability to sustain a human-like configuration while following the given end-effector position with regard to the different correspondence methods and explore the cause of bad postures with reference to the accuracy analysis of end-effector tracking.

Fig. 14a compares the elbow angle of the correspondence method wrist-closest-to-human (dotted line) with the wrist-elbow-in-line method (dashed line). The accuracy of end-effector tracking for these

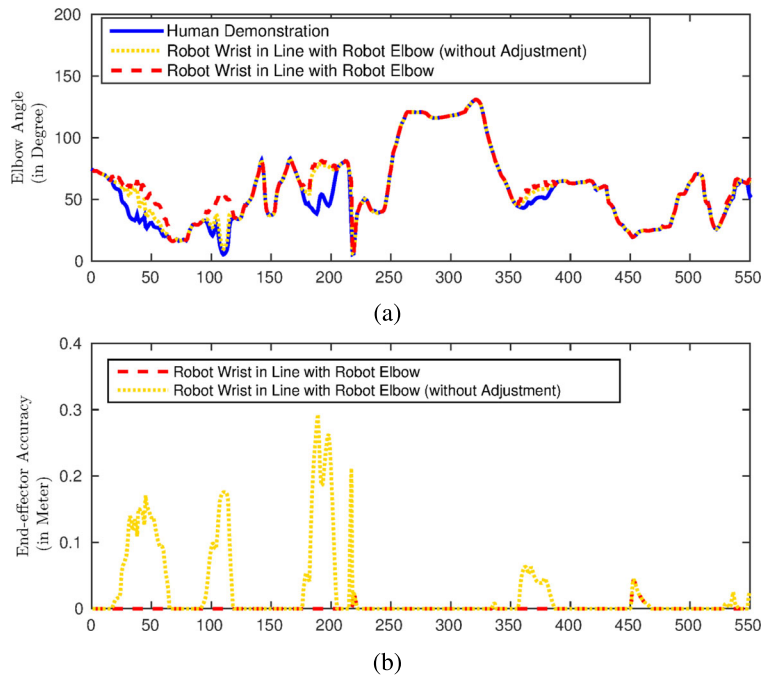

Fig. 16 Comparison of configuration adjustment effect for the wrist-elbow-in-line method: the robot's wrist in line with the elbow key position of robot with configuration adjustment vs. without adjustment. (**a**) and (**b**) show the elbow angle and the end-effector accuracy comparison respectively

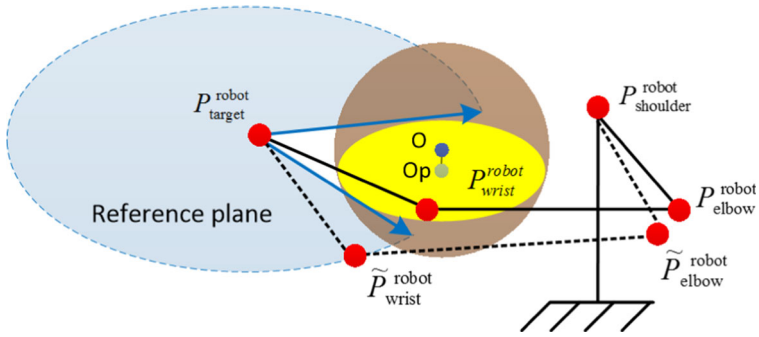

Fig. 17 Obstacle avoidance algorithm for wrist key position of the robot. The *yellow* disc is the intersection of reference plane and the spherical obstacle. *Blue* arrows are the boundary of feasible wrist positions without collision

two methods is illustrated in Fig. 14b. To some extent, the wrist key position of robot in the reference plane facilitates to find a suitable elbow solution with similar elbow angle. Because of the volatile human demonstration data in particular at the wrist position, the wrist key position of robot obtained from the wrist-closest-to-human method always falls out of the reference plane. And it is much easier to reach the joint limit of q_6 or q_2 in this case, as Fig. 5b exemplified. Then the elbow must rotate when searching a valid IK solution, which changes the human-likeness of the configuration to some extent. In addition, the adjustment can cause floating points in area 1 of Fig. 14a and result in a loss of accuracy in area 2 of Fig. 14b, if no

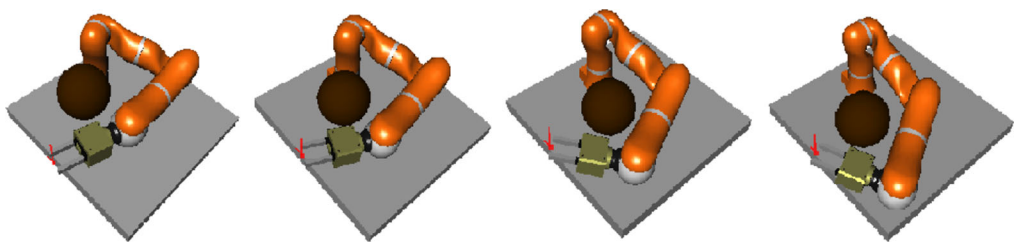

(a) Robot motion during obstacle avoidance given smame key positions of human demonstration

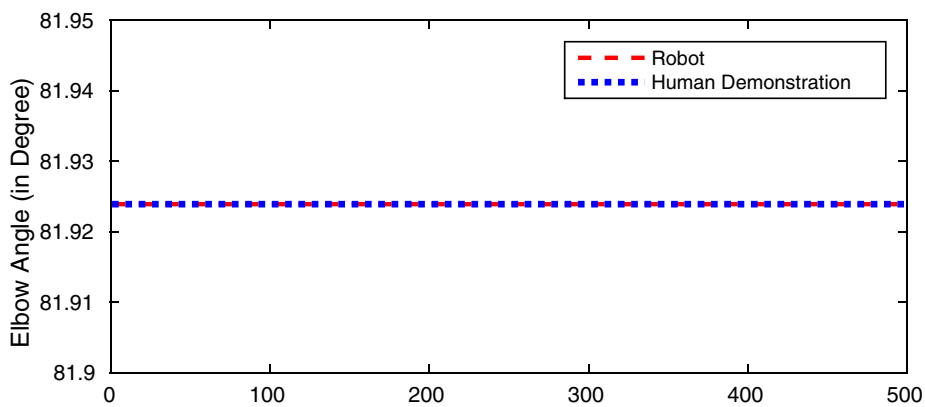

(b) Recorded elbow angle of robot arm during obstacle avoidance

Fig. 18 The elbow of robot maintains a similar configuration to human while the wrist of robot adjust to avoid the spherical obstacle nearby

suitable solution can be found. In area 3 of Fig. 14b, the target position is out of the robot's workspace after the scaling procedure, which causes not only a large error in accuracy in this area for both methods but results in an abrupt posture change for the wrist-closest-to-human method, see Fig. 5c. Overall, these two seemingly very similar correspondence methods display significantly different performance. In effect, the wrist-elbow-in-line method is much more stable.

To mediate the sometimes inevitable inconsistencies in the captured data from human demonstrations, especially at the wrist position, it is assumed that the elbow key position of human is in line with human wrist, as shown in Fig. 4. Then for decreasing the effect of low quality demonstration data at the wrist position in the wrist-closest-to-human method, the elbow of human demonstration can be used instead to solve for the position of the robot wrist. The respective elbow angle and end-effector accuracy are shown in Fig. 15. In this case, the main difference between these two methods is the priority between the wrist and the elbow key positions during configuration correspondence. In the wrist-elbow-in-line method, the elbow key position of robot has priority over the wrist, where the wrist is easily obtained according to the elbow position. On the contrary, in this new wrist-closest-to-human method using the human elbow instead of the wrist, first the wrist key position of robot is computed, and then the solution for the elbow. Even though as compared with Fig. 14, the dotted line is much stable, this method still results in low accuracies and big configuration changes at some points. There still remains the unsolved problem of abrupt posture changes in the area 3 of Fig. 15, that is, the robot's elbow is in the opposite direction of the elbow key position of human as Fig. 5c. So the sum of elbow angles of robot and human demonstration is close to 180 degrees without any configuration adjustment in this area. Through a configuration adjustment, a suitable elbow position is found for a valid IK solution in area 4 but with abrupt posture changes. At point 5 and 6 it fails to find a possible solution for the elbow and q_2 is set to its limit value because it exceeds the joint limit, which results in a low accuracy of end-effector and a loss of human-likeness.

In Fig. 16, it is easy to see that the end-effector accuracy significantly be improved after adjustment of the wrist-elbow-in-line method. But it has a bigger elbow angle difference to the human demonstration because the robot elbow needs to rotate to search for a valid IK solution.

In summary, the correspondence method with robot palm, wrist and elbow in line (wrist-elbow-in-line) combines better human-likeness with higher end-effector accuracy, even in the case of low quality of demonstration data. Still problematic is that because the human and robot arms have different joint limits and lengths, the configuration of the robot cannot follow the human arm posture well in areas near the joint limits of the robot and cannot be controlled as desired outside the reachable workspace of the human arm. We envisage that in future work machine learning could be combined with our approach to enable the robot to manipulate in a natural and human-like fashion for its entire workspace, by means of generalization to postures that are out of the human arm workspace.

4.3 Extension for Obstacle Avoidance

Finally, we exploit the flexibility of the wrist in order to add some obstacle avoidance algorithm in the wrist-elbow-in-line correspondence method. For simplicity, we consider only spherical obstacles. The avoidance algorithm is illustrated in Fig. 17, where O is the center of obstacle, O_p is its the projection in the reference plane, P is the key position of the robot after adjustment for obstacle avoidance and the blue dotted line indicates feasible solutions for the wrist. The value of the elbow angle is recorded while moving the spherical obstacle from position (-0.15, 0.15, 0.2) to position (-0.35, 0.3, 0.4) in meter around the wrist position given the same key positions of the human. From an intuitive point of view in Fig. 18a, it seems that the robot elbow always falls in the same plane to keep human-like posture while the wrist position adjusts to avoid the sphere obstacle. And the elbow angle remains constant 81.924° as in the human demonstration in Fig. 18b, which quantitatively verifies that the wrist flexibility can be used to maintain human-likeness of the robot posture while avoiding the obstacle.

5 Conclusions

Considering the requirement of human-friendly robot motion for everaday life tasks, a simple formulation

for human-like motion generation of a partially constrained redundant manipulator has been described in this paper. Based on the similarity in the kinematic structure between the human and the robot arm, the elbow and wrist joint positions in task space are used as configuration parameters for the robot arm to generate human-like movement. Thus the redundancy of robot arm is utilized to find a human-like configuration, which is obtained by means of an analytical solution of the inverse kinematics. The proposed method is tested with a 7-DOF robot arm, and motions in simulation are compared with the ones of human demonstration.

The main difference and advantage of key positions compared with conventional configuration control methods is that redundancy is resolved at position level in task space. Thereby, this approach provides a novel mixture of utilizing task and joint space for redundancy resolution. In principle, even for higher degrees of redundancy for instance in a full body humanoid robot, a similar approach could be derived, however must be left to future work.

Based on this idea, an analytical inverse kinematics solver is derived with relative ease, assuming that valid key positions are given. The key element to make this approach effective for imitation of human motion is to solve the correspondence problem to obtain valid key positions. It turns out, somewhat surprisingly, that a subtle difference in the correspondence method has a relatively large impact on the robustness of the method. It is worth mentioning that the method could be extended to obstacle avoidance where the human and robot arms are within their link lengths and joint limits and configurations without collision are natural for users.

Because link lengths and joint limits differ between a human and a robot arm, the robot would need to learn the ability of human-like configuration generation from human demonstration and generalize it over the whole workspace of robot. So the next step of this research will focus on the combination of this approach and machine learning to enable robot to perform new tasks in a natural human-like fashion for the entire workspace. And further research is currently conducted to develop an intuitive interface based on the idea of key positions in order to ease the control of a redundant robot for users and to satisfy much more possible applications.

Acknowledgment The authors wish to thank the colleagues in the Research Institute for Cognition and Robotics (CoR-Lab), especially C. Emmerich for supporting the simulation system for the experiment. Fruitful discussions with F. Reinhart are gratefully acknowledged. The first author benefits from a Doctoral Scholarship provided by China Scholarship Council (CSC) and the major subject of Beijing Science and Technology (D141100003614002). The experimental research was carried out while both authors were with the CoR-Lab.

References

1. Dragan, A., Srinivasa, S.: Familiarization to robot motion. In: ACM/IEEE International Conference on Human-Robot Interaction, pp. 366–373 (2014)
2. Galicki, M.: Generalized Kinematic Control of Redundant Manipulators, Springer London (2007)
3. Leeper, A., Hsiao, K., ciocarlie, M., Sucan, I.: Methods for collision-free arm teleoperation in clutter using constraints from 3d sensor data (2015)
4. Shimizu, M., Kakuya, H., Yoon, W.K., Kitagaki, K.: Analytical inverse kinematic computation for 7-DOF redundant manipulators with joint limits and its application to redundancy resolution. IEEE Trans. Robot. **24**(5), 1131–1142 (2008)
5. Toussaint, M., Gienger, M., Goerick, C.: Optimization of sequential attractor-based movement for compact behaviour generation. In: EEE-RAS International Conference on Humanoid Robots, pp. 122–129 (2007)
6. Sciavicco, L., Siciliano, B.: A solution algorithm to the inverse kinematic problem for redundant manipulators. IEEE J. Robot. Autom. **4**(4), 403–410 (2010)
7. Skoglund, A., Iliev, B., Palm, R.: Programming-by-demonstration of reaching motions—a next-state-planner approach. Robot. Auton. Syst. **58**(5), 607–621 (2009)
8. Mühlig, M., Gienger, M., Steil, J.J.: Interactive imitation learning of object movement skills. Auton. Robot. **32**(2), 97–114 (2012)
9. Liarokapis, M.V., Artemiadis, P.K., Bechlioulis, C.P., Kyriakopoulos, K.J.: Directions, methods and metrics for mapping human to robot motion with functional anthropomorphism: A review (2013)
10. Riley, M., Ude, A., Atkeson, C.G., Riley, M., Ude, A., Atkeson, C.G.: Methods for motion generation and interaction with a humanoid robot: Case studies of dancing and catching. In: Proceedings of the Workshop on Interactive Robotics and Entertainment, pp. 35–42 (2000)
11. Albrecht, S., Ramirez-Amaro, K., Ruiz-Ugalde, F., Weikersdorfer, D., Leibold, M., Ulbrich, M., Beetz, M.: Imitating human reaching motions using physically inspired optimization principles. In: 2011 11th IEEE-RAS International Conference on Humanoid Robots (Humanoids), pp. 602–607 (2011)
12. Pollard, N.S., Hodgins, J.K., Riley, M.J., Atkeson, C.G.: Adapting human motion for the control of a humanoid robot. In: Proceedings of the IEEE International Conference on Robotics and Automation, May 2002, pp. 1390–1397 (2002)

13. Seraji, H.: Configuration control of redundant manipulators: theory and implementation. IEEE Trans. Robot. Autom. **5**(4), 472–490 (1989)
14. Kim, S., Chang, H.K., Park, J.H.: Human-like arm motion generation for humanoid robots using motion capture database. In: IEEE/RSJ International Conference on Intelligent Robots and Systems, pp. 3486–3491 (2006)
15. Lopes, M., Santos-Victor, J.: Visual learning by imitation with motor representations. IEEE Transactions on Systems, Man, and Cybernetics, Part B (Cybernetics) **35**(3), 438–449 (2005)
16. Liarokapis, M.V., Artemiadis, P.K., Kyriakopoulos, K.J.: Mapping human to robot motion with functional anthropomorphism for teleoperation and telemanipulation with robot arm hand systems **8215**(2), 2075–2075 (2013)
17. Azad, P., Asfour, T., Dillmann, R.: Toward an unified representation for imitation of human motion on humanoids. In: IEEE International Conference on Robotics and Automation, pp. 2558–2563 (2007)
18. Asfour, T., Dillmann, R.: Human-like motion of a humanoid robot arm based on a closed-form solution of the inverse kinematics problem. In: Ieee/rsj International Conference on Intelligent Robots and Systems, vol. 2, pp. 1407–1412 (2003)
19. Santis, A.D., Pierro, P., Siciliano, B.: The multiple virtual end-effectors approach for human-robot interaction (2006)
20. Santis A. D., Siciliano, B.: Reactive collision avoidance for safer human-robot interaction. IARP/IEEE Ras/euron Workshop on Technical Challenges for Dependable Robots in Human Environments, 2007. [Online] Available: http://www.phriends.org/papers.htm
21. Ciocarlie, M., Hsiao, K., Jones, E.G., Chitta, S., Rusu, R.B., Şucan, I.A.: Towards reliable grasping and manipulation in household environments. Springer Tracts in Advanced Robotics **79**, 241–252 (2014)
22. Artemiadis, P.: Closed-Form Inverse Kinematic Solution for Anthropomorphic Motion in Redundant Robot Arms. Advances in Robotics & Automation **02**(03) (2013). [Online]. Available: http://www.omicsgroup.org/journals/closedform-inverse-kinematic-solution-for-anthropomorphic-motion-in-redundant-robot-arms-2168-9695.1000110.php?aid=21589
23. Zanchettin, A.M., Bascetta, L., Rocco, P.: Achieving humanlike motion: Resolving redundancy for anthropomorphic industrial manipulators. IEEE Robotics and Amp, Amp Automation Magazine **20**(20), 131–138 (2013)
24. Billard, A., Grollman, D.: Robot learning by demonstration, vol. 8 (2013)
25. Kuba, K., Tomita, T.: Teleoperation for learning by demonstration: Data glove versus object manipulation for intuitive robot control. International Congress on Ultra Modern Telecommunications and Control Systems and Workshops, 346–351 (2014)
26. Kirstein, F., Fischer, K., Lvason, D.: Human embodiment creates problems for robot learning by demonstration using a control panel. In: ACM/IEEE International Conference on Human-robot Interaction, pp. 212–213 (2014)
27. Chiaverini, S., Oriolo, G., Walker, I.D.: Kinematically Redundant Manipulators, pp. 245–268. Springer, Heidelberg (2007)
28. Kim, H., Miller, L.M., Byl, N., Abrams, G.M., Rosen, J.: Redundancy resolution of the human arm and an upper limb exoskeleton. IEEE transactions on bio-medical engineering **59**(6), 1770–9 (2012)
29. A Roundabout Route to Geometric Algebra. Springer, New York (2006)
30. Emmerich, C., Nordmann, A., Swadzba, A., Steil, J.J., Wrede, S.: Assisted gravity compensation to cope with the complexity of kinesthetic teaching on redundant robots. In: Proceedings - IEEE International Conference on Robotics and Automation, pp. 4322–4328 (2013)
31. Wrede, S., Emmerich, C., Grünberg, R., Nordmann, A., Swadzba, A., Steil, J.J.: A user study on kinesthetic teaching of redundant robots in task and configuration space. Journal of Human-Robot Interaction **2**(1), 56–81 (2013)

Weihui Liu received the B.S. degree in Mechanical Engineering and Automation from Beihang University in 2011. From Sep, 2014 to Oct, 2015 she was a Visiting Ph.D. Researcher with Institute for Cognition and Robotics (CoR-Lab), Bielefeld University. Her research interests are in robotics, especially in redundant manipulators and human-robot interaction. She is currently a Ph.D. candidate of Robotics Institute, Beihang University.

Diansheng Chen received his PhD degree in Mechanical Engineering and Automation from Jilin University in 2003. From 2003 to 2006 he was a Postdoctoral Researcher with the Department of Mechanical Engineering and Automation, Beihang University. He is currently a full professor and director of Intelligent Technology and Robotics (ITR) of Robotics Institute, Beihang University. His research interests are fields of service robotics, bio-robotics, and intelligent mechatronics control technology.

Jochen Steil received the B.S. in mathematics and a Ph.D. in Computer Science from the University of Bielefeld, Germany, in 1993 and 1999, respectively and received the venia legendi in Neuroinformatics in 2006. Between 2007-2016, he has been managing director of the Institute for Cognition and Robotics (CoR-Lab) at Bielefeld University and scientific board member of the Cognitive Interaction Technology Excellence Center (CITEC). Research stays included one year at the St. Petersburg Electrotechnical University, Russia, time with the Honda Research Institute Europe (Offenbach) and a temporary appointment at Oxford Brookes University, where currently he is a visiting professor. From 2016, J. Steil has been full professor in Robotics and Process Control at the Technische Universität Braunschweig. He has published more than 150 papers in his research areas of robotics, human-machine interaction, and in particular neural learning systems.